Schistosoma mansoni extracellular vesicles and their impact on the immune system: glycosylated messengers in host-pathogen communication

Kuipers, M.E.

Chapter 6

DC-SIGN mediated internalisation of glycosylated extracellular vesicles from *Schistosoma mansoni* increases activation of monocyte-derived dendritic cells

Marije E. Kuipers, Esther N.M. Nolte-'t Hoen, Alwin J. van der Ham, Arifa Ozir-Fazalalikhan, D. Linh Nguyen, Clarize M. de Korne, Roman I. Koning, John J. Tomes, Karl F. Hoffmann, Hermelijn H. Smits*, Cornelis H. Hokke*
*These authors contributed equally

Journal of Extracellular Vesicles, 2020

PMID: 32489529

DOI: 10.1080/20013078.2020.1753420

Abstract

Helminths like *Schistosoma mansoni* release excretory/secretory (ES) products that modulate host immunity to enable infection. Extracellular vesicles (EVs) are among these ES products, yet molecular mechanisms and functionality of *S. mansoni* EV interaction with host immune cells is unknown. Here we demonstrate that EVs released by *S. mansoni* schistosomula are internalised by human monocyte-derived dendritic cells (moDCs). Importantly, we show that this uptake was mainly mediated via DC-SIGN (CD209). Blocking DC-SIGN almost completely abrogated EV uptake, while blocking mannose receptor (MR, CD206) or dendritic cell immunoreceptor (DCIR, CLEC4A) had no effect on EV uptake. Mass spectrometric analysis of EV glycans revealed the presence of surface N-glycans with terminal Galβ1-4(Fucα1-3)GlcNAc (Lewis X or Le^x) motifs, and a wide array of fucosylated lipid-linked glycans, including Le^x, a known ligand for DC-SIGN. Stimulation of moDCs with schistosomula EVs led to increased expression of costimulatory molecules CD86 and CD80 and regulatory surface marker PD-L1. Furthermore, schistosomula EVs increased expression of IL-12 and IL-10 by moDCs, which was partly dependent on the interaction with DC-SIGN. These results provide the first evidence that glycosylation of *S. mansoni* EVs facilitates the interaction with host immune cells and reveals a role for DC-SIGN and EV-associated glycoconjugates in parasite-induced immune modulation.

Introduction

Schistosoma mansoni is one of the major helminth parasites of humans with over 200 million people infected[1,2]. In the initial phase of infection, schistosome larvae (cercariae) penetrate the skin of the host and transform into schistosomula. These schistosomula larvae will migrate to the circulatory system, develop into adult worms that mate and lay eggs[3]. *S. mansoni* can live up to 10 years in its host because it has developed successful mechanisms to evade immune responses. To establish this immune evasion, the parasite releases excretory/secretory (ES) products that act on the host immune system[4]. Among these ES products are extracellular vesicles (EVs) and evidence is accumulating that parasite-derived EVs contribute to parasite-host interaction[5]. The molecular composition of EVs from *S. mansoni* larvae and adult worms life stages has been partially characterized[6–8], but the interaction of their EVs with host cells remains unexplored.

For schistosomes to initiate and maintain infection, modulating host innate and adaptive immune responses is crucial[9]. Mouse models have shown that cercarial penetration triggers migration of innate antigen presenting cells (APCs), such as macrophages and dendritic cells (DCs), towards the skin draining lymph nodes[10]. These APCs have upregulated costimulatory molecules, like CD86 and major histocompatibility complex (MHC) class II, which are important for initiating adaptive immune responses. *In vitro* stimulation of mouse bone marrow-derived DCs (BMDCs) with ES from schistosomula shows a similar pattern: increased costimulatory molecules and MHC class II expression and increased pro-inflammatory cytokine release (IL-6, IL-12, and TNF-α)[11]. Furthermore, cercarial secretions can upregulate the expression of IL-10 and programmed death ligand (PD-L)1 and 2 in human monocyte-derived (mo)DCs, suggesting that the parasite additionally utilizes regulatory pathways to dampen adaptive immune responses[12]. Relatively little is known about the exact molecular or structural components derived from schistosomula that induce immunomodulatory effects. Thus far, it has been shown that recombinant tetraspanins, transmembrane proteins associated to adult worm EVs[13], induce IL-10 and Th1 cytokine responses by peripheral blood mononuclear cells[14]. Whether schistosomula EVs have similar effects on human DCs has not been investigated.

Studies exploring the molecular content of schistosomula ES have shown that part of the cytokine responses by mouse macrophages and whole blood of infected individuals is induced by glycosylated antigens in the ES[15,16]. Schistosome glycoconjugates can be recognized by host pathogen recognition receptors (PRRs) on APCs, in particular the C-type lectin receptors (CLRs) such as the mannose receptor (MR, CD206)[17], dectin-1/2[18], dendritic cell immunoreceptor (DCIR, CLEC4A, CD367)[19], and dendritic cell-specific ICAM-3-grabbing nonintegrin (DC-SIGN,

CD209)[20]. A well-known immunogenic glycan-motif, Galβ1-4(Fucα1-3)GlcNAc or Lewis X (Le^X), is present on glycoproteins in schistosomula and egg ES and can be recognized by DC-SIGN[21] as well as MR[22], leading to different effects depending on the structural context of the Le^X motif. Pathogen-associated molecular patterns (PAMPs) containing high-mannose (oligomannose) structures, which form ligands for MR and DC-SIGN[23] have also been found on glycoproteins in ES from schistosomes[24]. This raises the question whether schistosomula EVs expose glycans instrumental in targeting to host immune cells and whether these EV-associated glycans play a role in modifying subsequent immune responses. While it is known that mammalian EVs contain glycoconjugates, publications on the structure and function of EV glycans are very limited so far[25–29].

In order to gain insights into the interaction of schistosome EVs with the immune system we studied the interaction of schistosomula EVs with human moDCs and found that the EVs are internalised mainly via DC-SIGN. We show that N-glycans on the surface and glycolipids of the EVs contain DC-SIGN ligands, including Le^X. Furthermore, we demonstrate that these EV preparations increase the activation status of moDCs, affecting both immunostimulatory and immunoregulatory pathways which were partly dependent on the interaction with DC-SIGN. Our study provides evidence for a specific CLR-mediated uptake of EVs that substantiates the importance of EV-associated glycoconjugates in pathogen-host interaction.

Materials and Methods

Schistosomula culture

Infected *Biomphalaria glabrata* snails were incubated in water at 30 °C for 2 h to shed cercariae of the Puerto Rican-strain of *S. mansoni* by exposure to light. The collected cercariae in water were stored on ice for 1.5 h to immobilize them and were subsequently pelleted by centrifugation at 440 × *g*. After removal of the supernatant, 12 ml of pre-warmed (37 °C) DMEM (Dulbecco's Modified Eagle Medium, high glucose with L-glutamine, Lonza, Basel, Switzerland) supplemented with 200 U/ml penicillin and 200 µg/ml streptomycin (Sigma-Aldrich, St. Louis, MO, USA), was added to transform the cercariae to schistosomula by providing mechanical force via pipetting and incubating for 20 min at 37 °C[30]. Cercarial bodies were separated from their tails using an orbital shaker. The collected schistosomula were resuspended in DMEM at a concentration of 7,500 schistosomula/ml and cultured in 25 cm^2 polystyrene flasks (Greiner Bio-One, Alphen a/d Rijn, The Netherlands) at 37 °C and 5% CO_2 for 72 h.

EV isolation and staining

Schistosomula ES products were enriched for EVs by differential centrifugation as previously described, with minor modifications[6]. Briefly, the collected culture supernatant (9-34 ml per culture, 7,500 schistosomula/ml) was centrifuged in 15 ml tubes (Greiner Bio-One) twice at 500 × *g* (k-factor 115,790.8) for 2 min (4 °C) (SX4750A rotor and an Allegra X-15R centrifuge) (Beckman Coulter, Brea, CA, USA) with low brake to remove remaining parasites. To remove any residual debris, the supernatant was subsequently centrifuged at 700 × *g* (k-factor 82,764.4) for 20 min (4 °C, low brake). Next, an EV-enriched pellet was obtained by centrifugation of the supernatant at 31,000 rpm (average around 120,000 × *g*, k-factor 216.3) for 80 min at 4 °C (max. acceleration and brake), followed by three wash steps with cold phosphate buffered saline (PBS) (B. Braun, Melsungen, Germany) in thinwall polypropylene tubes using an SW41 Ti rotor and an Optima XE-90 ultracentrifuge (Beckman Coulter). For binding/uptake experiments, EVs were stained with PKH26 (Sigma-Aldrich) after the first ultracentrifugation step by addition of 80 µl Diluent C to the resuspended EV-enriched pellet and incubation of 93 µl diluted PKH26 (1.5 µl in 100 µl Diluent C) for 3 min at RT before addition of 11 ml PBS. Unconditioned culture medium incubated without parasites was processed (and stained) following the same procedures and was used as (dye) control. EV-enriched pellets (from 66,300-253,200 schistosomula) for *in vitro* experiments were resuspended in 510 µl PBS, for transmission electron microscopy (TEM) and glycan analysis in 100 µl PBS, and for cryo EM in 40 µl PBS. All were stored at -80 °C until further use except for 1 cryo EM sample, which was processed directly after EV isolation. We have submitted all relevant data of our experiments to the EV-TRACK knowledgebase (EV-TRACK ID: EV190032)[31].

Transmission electron microscopy

EV preparations were generated in Leiden and visualized by TEM at Aberystwyth University, as described previously[6]. Briefly, 10 µl of EV-enriched sample was fixed with an equal volume of 4% glutaraldehyde, adsorbed onto Formvar/carbon-coated copper grids (Agar scientific, Stansted, UK) for 40 min, and subsequently contrast stained with 2% uranyl acetate (pH 4) for 10 min. Processed samples were then visualized on a Jeol 1010 transmission electron microscope operated at 80 kV. Images were recorded with a Kodak MegaPlus camera Model 1.4i, other than the addition of scale bars, no further image processing was done. Sizes were measured by hand using Fiji/ImageJ software[32].

Nanoparticle tracking analysis (NTA)

EV-enriched suspensions were diluted 1:100 in PBS (to obtain 25-100 particles per frame at camera level 16) before analysing the concentration and size distribution by nanoparticle tracking analysis (NTA) using a NanoSight NS500 (Malvern Panalytical, Malvern, UK) equipped with an sCMOS camera. For each EV-enriched pellet, three videos of 30 seconds were recorded on three different camera levels: 12, 14, and 16. The analysis was done with NTA3.3 software and a detection threshold of 5. The average particle concentration of nine videos per EV-enriched sample, after subtraction of the NTA background data from PBS alone, was used for further experiments. We additionally measured the protein concentration of the EV-enriched pellets with microBCA according to the manufacturers protocol (Pierce, Thermo Fisher Scientific, Waltham, MA, USA).

Cryo electron microscopy

Previously frozen or freshly isolated EV preparations (EV from 86,00-112,00 schistosomula in 40 µl PBS) were visualized by cryo EM. Copper EM grids supporting a carbon film with regularly spaced 2 micron holes (R2/2, Quantifoil, Jena, Germany) were glow-discharged in air at 0.2 mbar for 2 min at 20 mA (EMITECH K950X with glow discharger unit). A 3 µl drop of sample was applied to the grid and transferred into the environmental chamber of a Leica EM grid plunger (Leica Microsystems, Wetzlar, Germany) operating at RT and between 92% and 94% humidity. Excess sample was blotted away for 1 second using filter paper (Whatman no.1) and without waiting plunged into a mixture of ethane/propane (63/37 v/v) cooled with liquid nitrogen to -193 °C. After vitrification, grids were stored under liquid nitrogen and transferred into a cryo holder (type 626, Gatan, Germany). In total 238 cryo-EM projection images were recorded by 1 second exposures at spot 5 on a FEI Tecnai F12 at 120 kEV on a 4k × 4k CCD camera (Eagle, Thermo Fisher Scientific) at a magnification of 13,500 × (0.85 nm pixel size) and a defocus value ~ -8 microns. Size measurement was performed by hand using Fiji/ImageJ software[32]. After removing double images and images with no EVs, 233 images were used to measure a total of 1056 EVs, which were subsequently quantified in segments of 20 nm (i.e. 21-40 nm, 41-60 nm, 61-80 nm...861-880 nm, 881-900 nm).

Human monocyte-derived dendritic cells (moDCs)

Venous blood of healthy volunteers who provided informed consent, approved by the Institutional Review Board of Leiden University Medical Centre, was used to isolate monocytes and differentiate to moDCs as previously described[33]. Immature DCs were harvested on day 5 or 6, counted, seeded at 5×10^4 cells/well in a 96

well flat-bottom plate, and rested overnight at 37 °C and 5% CO_2. Subsequently, cells were stimulated with or without a pre-incubation of 30 min with 10 mM EGTA (Sigma-Aldrich), 20 µg/ml αDC-SIGN/CD209 (clone AZN-D1, custom order without sodium-azide) (Beckman Coulter), 20 µg/ml αMR/CD206 (clone 15-2) (BioLegend, San Diego, CA, USA), 20 µg/ml αDCIR/CLEC4A (clone 111F8.04, Dendritics, Novus Biologicals, Centennial, CO, USA), and 20 µg/ml mouse IgG1 isotype control (clone P3.6.2.8.1) (Invitrogen, Thermo Fisher Scientific) in the presence of αFcgammaR-binding inhibitor (eBioscience, Invitrogen) and in the presence or absence of the maturation factors IL-1β (25 ng/ml) (BioLegend) and TNF-α (50 ng/ml) (Sino Biological, Beijing, P.R. China) or LPS (100 ng/ml) (InvivoGen, San Diego, CA, USA). As a positive control for the αMR, PF-647-labelled recombinant omega-1 was used[22,34]. EV-enriched pellets were thawed only once and several EV batches were pooled before incubation with the cells (6×10^9 EV/ml or mentioned otherwise). To investigate the effect of surface de-N-glycosylation, EVs were incubated with or without peptide N-glycosidase F (PNGase F) (4 U/100 µl, Roche Diagnostics, Almere, The Netherlands) at 37 °C for 20 h before moDC incubation. Supernatants were collected from >85% $CD1a^+$ cell cultures after 24 h stimulation and IL-6 (Sanquin, Amsterdam, The Netherlands), IL-10 (BioLegend), and IL-12p70 (BD Biosciences, Franklin Lakes, NJ, USA) cytokine production was determined with ELISA according to the manufacturers protocols. Stimulated moDCs were washed, stained, and measured by flow cytometry on a FACSCanto II (BD Bioscience) and using the following antibodies: CD1a-BV421 (clone HI149) (BioLegend), HLA-DR-APC-eF780 (clone LN3) (eBioscience), PD-L2/CD273-FITC (clone MIH18) (Miltenyi Biotec, Bergisch Gladbach, Germany), CD86-FITC (clone 2331 (FUN-1)), CD40-APC (clone 5C3), CD80-V450 (clone L307.4), PD-L1/CD274-PE-Cy7 (clone MIH1) (all BD Bioscience) with the addition of Fc receptor binding inhibitor (eBioscience) and Aqua live/dead staining (Invitrogen). Flow cytometric measurements were analysed with FlowJo (version 10, BD Bioscience).

Confocal microscopy

5×10^4 moDCs/chamber were seeded onto poly-L-lysine (Sigma-Aldrich) coated coverslips of a 4 chamber glass bottom dish (ø35mm; Greiner Bio-One) for 24 h. Cells were pre-incubated with EGTA or αDC-SIGN+αFcgammaR-binding inhibitor as described above, incubated with PKH-labelled schistosomula EV-enriched pellets for 5 h, subsequently washed, and treated with Hoechst (Sigma-Aldrich). Images were taken at 37 °C and 5% CO_2 on a Leica TCS (true confocal scanning SP8 WLL (white light laser) microscope (Leica Microsystems). The sequential scanning mode was applied to image Hoechst (excitation: 405 nm, emission: 420-470 nm) and PKH26 (excitation: 561 nm, emission: 570-630 nm). For imaging the uptake of

EVs, a 63× objective (Leica HC PL APO 63×/1.40na OIL CS2) was used. The z-stacks were recorded and maximum projections of the recorded z-stacks were generated using the Leica software (LAS X version 1.1.0.12420; Leica Microsystems).

N-glycan and glycolipid-glycan analysis

For the N-glycan analysis, EV-enriched pellets (in PBS) from >100,000 cultured schistosomula were lyophilized, resuspended in 100 µl milliQ water, sonicated and subsequently reduced and denatured for 10 min at 95 °C with the addition of SDS and β-mercaptoethanol which were neutralized by adding NP-40 (Sigma-Aldrich). Full details on N-glycan isolation has been described previously[35]. N-glycans were released by PNGase F (4 U/100 µl) incubation for 24 h at 37 °C and cleaned up by collection in the flow through of reversed phase (RP) C18-cartridges (JT Baker, Phillipsburg, NJ, USA) followed by isolation on carbon cartridges (Supelclean ENVI-carb SPE, Sigma-Aldrich). In addition, directly after isolation, intact EV preparations in PBS were treated with PNGase F for 24 h at 37 °C to release directly accessible N-glycans (surface glycans). The total suspension was subsequently transferred to a thinwall polypropylene tube and topped up with PBS. The EVs were pelleted by ultracentrifugation at 42,000 rpm (average around 120,000 × *g*, k-factor 85.4) for 65 min at 4 °C (max. acceleration and brake) using a TLS-55 rotor and an Optima TLX (Beckman Coulter). Next, the supernatant containing the PNGase F released N-glycans was collected and these N-glycans were isolated with C18- and carbon-cartridges. The EV-enriched pellet without PNGase F accessible surface N-glycans was resuspended in PBS, lyophilized, sonicated, reduced, denatured, and treated with PNGase F to isolate remaining N-glycans as above.

For glycolipid-glycans analysis, EV-enriched pellets were lyophilized, resuspended in milliQ water, sonicated, and subjected to extraction with chloroform and methanol (MeOH). The upper phase was collected after sonication and centrifugation. Similar volume as collected was replaced with 50% MeOH and the previous steps were repeated twice. All collected upper phases of the extraction were applied to an RP C18-cartridge and flow-through and wash fractions were combined and applied to another C18-cartridge. Glycolipids were eluted from the cartridges with chloroform/MeOH/water and dried under a flow of nitrogen. The glycolipids were subsequently dissolved in 200 µl 50 mM sodium acetate with 0.1% sodium taurodeoxycholate hydrate (Sigma-Aldrich), sonicated, and heated to 60 °C for 10 min. 2 mU of recombinant endoglycoceramidase II (*Rhodococcus* sp.) (rEGCase II) (Takara-bio, Kusatsu, Shiga, Japan) was added to release the lipid-bound glycans. After 24 h at 37 °C, another 2 mU was added and the sample was incubated at 37 °C for another 24 h. The purification of released

lipid-glycans was performed as described for the N-glycans using RP C18- and carbon cartridges.

To support glycan structure assignments, part of the isolated N-glycans and glycolipid-glycans were additionally treated with hydrofluoric acid (HF), which removes labile substitutions including α1-3 linked fucoses. All isolated glycans were labelled with 2-aminobenzoicacid and purified by Biogel P10 (Bio-Rad, Hercules, CA, USA). The labelled glycans were measured by MALDI-TOF-MS with 2,5-dihydroxybenzoic acid (Bruker Daltonics, Bremen, Germany) as matrix using UltrafleXtreme mass spectrometers (Bruker Daltonics) in the negative-ion reflectron mode. When necessary, samples were cleaned up with ZipTip C18 (Merck Millipore, Burlington, MA, USA) before MALDI-TOF-MS. The obtained mass spectra were smoothed and the base-line was subtracted using FlexAnalysis (version 3.4, Bruker Daltonics). Glycan compositions were identified from the peak lists using GlycoWorkbench (Version 3)[36]. Peaks with a signal to noise ratio below 2 were excluded and masses are registered as deprotonated $[M-H]^-$. 2-AA was taken into account as a fixed reducing-end modification. For the interpretation of the relative most abundant signals for spectral assignments we used (when available) previously published structural data from *S. mansoni* glycans[35]. In the spectra, the structure of the most likely or most abundant isomer of the composition is indicated.

RNA extraction and qPCR analysis

Human moDCs were pre-incubated with or without αDC-SIGN, αMR, or IgG1 isotype and stimulated with IL-1β and TNF-α and schistosomula EV-enriched preparations as described above. After 6 h stimulation at 37 °C and 5% CO_2, cells were stored on ice for 10 min, harvested, washed with cold PBS, snap frozen, and stored at -80 °C till RNA extraction. RNA was extracted with the RNeasy Kit (Qiagen, Hilden, Germany) according to the manufacturer's protocol. RNA was quantified using NanoDrop 1000 Spectrophotometer (Thermo Fisher Scientific) and cDNA synthesis was performed on 0.2 µg RNA according to standard procedures. Primer Express (Applied Biosystems, Waltham, MA, USA) was used to design primers that were synthesized by Biolegio (Nijmegen, The Netherlands). Sequences of the primers were: β-actin_Forward(F): 5'- GCTACGAGCTGCCTGACGG-3'; β-actin_Reverse(R): 5'- CAGCGAGGCCAGGATGGAGCC-3'; β-2-M_F: 5'-TGCCGTGTGAACCATGTGA-3'; β-2-M_R: 5'-CCAAATGCGGCATCTTCAA-3'; RPLPO_F: 5'-GGCGACCTGGAAGTCCAACT-3'; RPLPO_R: 5'-CCATCAGCAC-CACAGCCTTC-3'; IL-10_F: 5'-ACCTGCCTAACATGCTTCGAG-3'; IL-10_R: 5'-CCAGCTGATCCTTCATTTGAAAG-3'; TNF-α_F: 5'-TCTTCTCGAACCCCGAGTGA-3'; TNF-α_R: 5'-CCTCTGATGGCACCACCAG-3'; IL-12p35_F: 5'-CTCCTGGACCACCT-

CAGTTTG-3'; IL-12p35_R: 5'-TTGTCTGGCCTTCTGGAGCA-3'. Quantitative real-time PCR (qPCR) was performed using CFX96 instruments (Bio-Rad Laboratories) and CFX Maestro (Bio-Rad) software. Technical duplicates with <1 C_q value difference were averaged and gene expression was calculated with the $\Delta\Delta C_q$ method using the average C_q of the reference genes β-actin, β-2-M, and RPLPO to normalize[37].

Statistical analyses

All data were analysed using a paired student t-test or repeated measures One-way ANOVA (P-values <0.05 were considered significant) with Tukey's or Dunnett's Multiple Comparison Test in GraphPad Prism 5.0 (GraphPad Software, Inc., La Jolla, CA, USA).

Results

Cryo electron microscopy reveals ultrastructural characteristics of schistosomula EVs

Schistosomula were cultured for 72 h and EV-enriched preparations were obtained from schistosomula ES by sequential (ultra)centrifugation steps. TEM confirmed isolation of vesicles in the size-range between 35 and 190 nm (Figure 1a-b). NTA analysis showed a size-range of 30-650 nm with a minor peak around 40 nm and three major peaks around 110, 160, and 350 nm (Figure 1c). Culture medium without parasites that was processed similarly (medium control) and PBS alone only showed minor peaks between 60 and 150 nm as NTA background (Figure 1c).

→ Figure 1. TEM, NTA and cryo EM measurement of schistosomula EVs

EV-enriched preparations analysed by transmission electron microscopy at 60,000 × (a) and 120,000 × magnification (b). Scale bars are 200 nm. EVs are pointed out with arrow heads, the small (<60 nm) structures (black arrows) in (b) are artefacts and were also observed in PBS only. In addition, EVs were analysed by nanoparticle tracking analysis (NTA) (c). The graph shows the average of 17 schistosomula EV-enriched preparations (black line), 10 medium controls (dark orange line), and 15 PBS (background) in which the preparations were resuspended (blue line), averages are shown with SEM (lighter areas). Cryo EM of EVs at 13,500 × magnification (d). Scale bars are 500 nm. The EV membrane and stretch of the filamentous structures are indicated in the middle pane with white dashed circles and black dashed circles, respectively. Right pane shows a close up of one EV with filaments. Quantification of the EV sizes excluding (EV diameter) or including (EV diameter + filaments) the thin filaments from a total of 1056 EVs (e). EM pictures are representative for four biological replicates.

The average particle concentration measured with NTA was 2.33E[10]/100,000 schistosomula and the average protein concentration of EV-enriched preparations was 6 µg/100,000 schistosomula.

Although the TEM images corresponded with previous observations[6], there was a discrepancy in the sizes measured with the TEM and NTA. Therefore, we

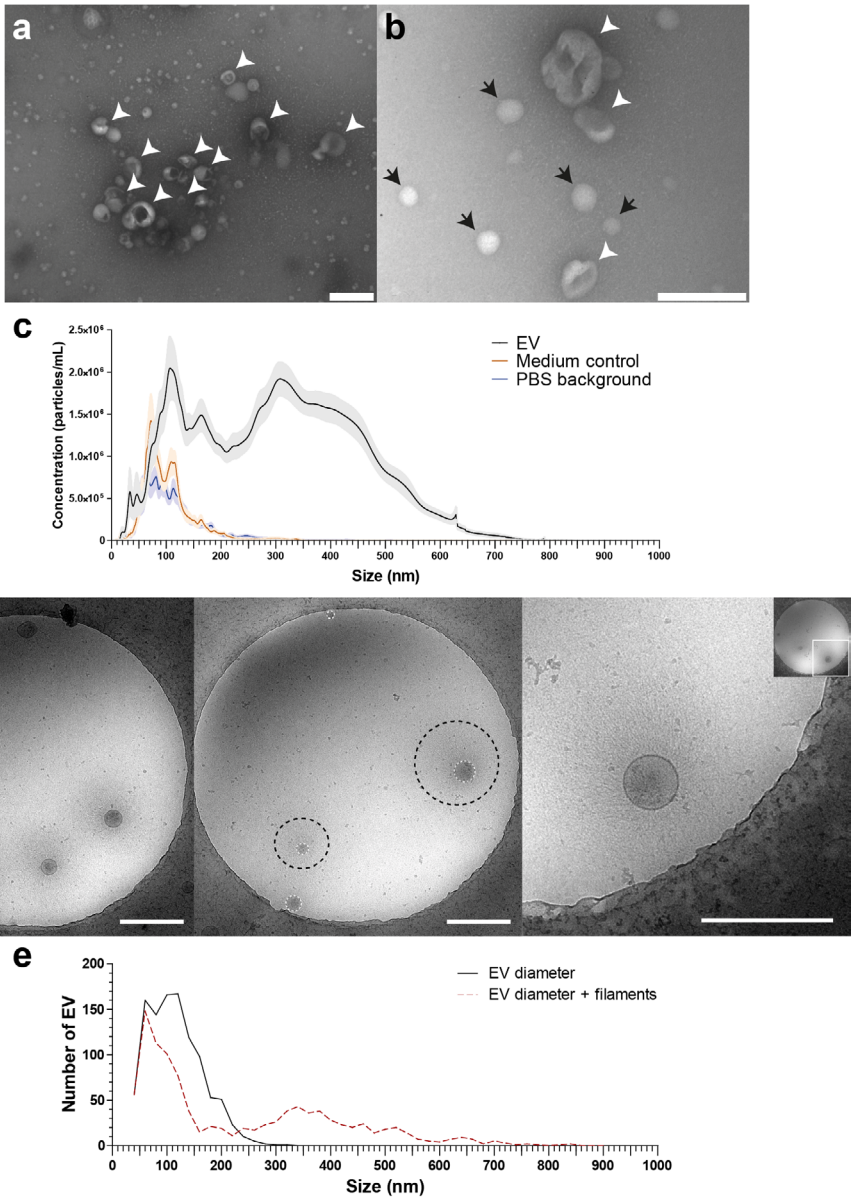

additionally analysed the EV preparations with cryo EM to visualise the near native state of the EVs and measure their size (Figure 1d). Interestingly, the cryo EM revealed thin filament-like structures covering the EV surface in 45.5% of all measured EV and in >70% of EVs when excluding EVs smaller than 100 nm. The filamentous structures ranged from 10 to 340 nm in length (average length of 128.5 nm) additional to the size of the EV diameter to the EV membrane (Figure 1e). These surface structures were most likely lost during the sample preparation for negative stained TEM (Figure 1a) and thus not observed, while NTA size measurement did include these structures as shown by similar size ranges between NTA and cryo EM.

Internalisation of schistosomula EV by human moDCs is calcium dependent

To investigate the interaction of schistosomula EVs with human moDCs, EVs were first labelled with the fluorescent dye PKH26. MoDCs (0.25E^{6} moDC/ml) were incubated with a maximum of 6E^{9} EV/ml, which is equivalent to approximately 10 moDCs receiving the number of EVs released by one schistosomulum during three days of culture. After 2 h of incubation, there was a dose-dependent increase in EV binding/uptake by the CD1a^{+} moDCs indicated by an increased geometric mean fluorescence intensity (geoMFI) relative to cells in medium only (Figure 2). Furthermore, the fluorescence of cells incubated with dye control was unchanged, indicating that the increase in MFI was due to binding/uptake of labelled EVs and not due to dye aggregates[38]. EV binding/uptake by moDCs did not change due to stimulation of the cells with LPS or in the presence of IL-1β+TNF-α. Incubation at 4 °C instead of 37 °C did not lead to binding/uptake of EVs by the moDCs (Figure 2), suggesting that the interaction with and uptake of the schistosomula EVs by target cells are active processes. We visually confirmed that EVs were internalised by moDCs with confocal microscopy (Figure 2c).

MoDCs are known to express C-type lectin receptors that bind glycan motifs present on schistosome ES components in a calcium dependent manner[39]. To investigate whether moDCs also recognise schistosomula EVs via CLR-glycan motif interactions, moDCs were incubated with fluorescently labelled EVs in the presence of the calcium chelator EGTA and subsequently analysed by flow cytometry and confocal microscopy (Figure 2d-e). Pre-incubation of EGTA almost completely abrogated the fluorescence signal and EV internalisation of moDCs compared to EV-exposed moDCs without EGTA pre-incubation, indicating calcium dependent interaction with moDCs such as CLRs. Next, when EGTA was added after incubation with EVs in order to remove EVs bound to CLRs, this resulted in

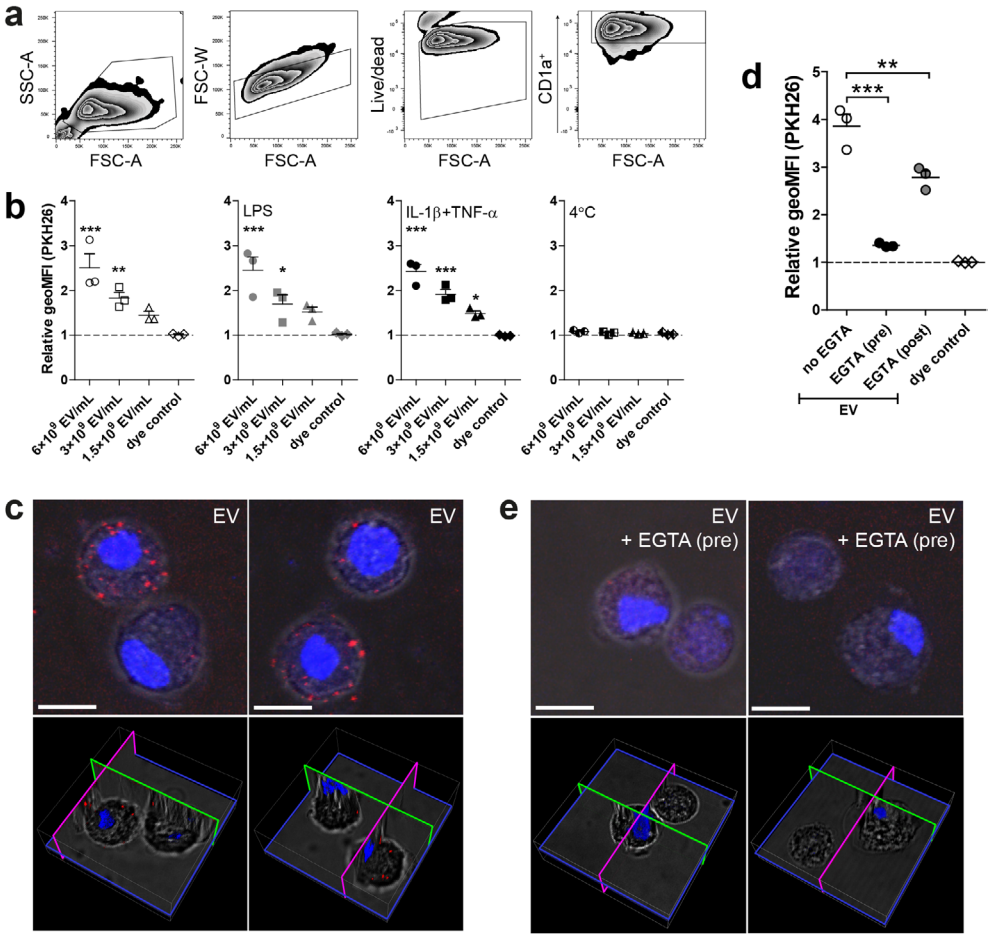

Figure 2. Dose dependent uptake of schistosomula EVs by human moDC is temperature and calcium dependent

Measured PKH26 fluorescence (PKH26 labelled EVs) of CD1a⁺ cells was obtained via gating as pictured in (a). The geoMFI (geometric mean fluorescent intensity) of PKH26 is shown relative to unstimulated cells (b). MoDC from three donors. EV uptake visualized by confocal microscopy (c). Images show maximum projections (top panels) and 3D visualizations (bottom panels) of recorded z-stacks of two different fields. PKH26-labelled EVs are stained in red and the nuclei in blue (Hoechst). Selected pictures are representative for three donors. Human moDC incubated with EVs with either EGTA added pre- or post-incubation (d). Confocal images of moDC pre-treated with EGTA followed by EV incubation (e). Scale bars are 10 µm. Mean±SEM *$p < 0.05$, **$p < 0.01$, ***$p < 0.001$, using repeated measures ANOVA with Dunnett's Multiple Comparison Test compared to cells in medium only (b) or repeated measures ANOVA with Tukey's Multiple Comparison Test (d). SSC-A, side-scatter; FSC-A, forward-scatter

only a minor reduction of fluorescence signal (Figure 2d), confirming that most of the EVs were internalised by moDCs rather than bound to the surface.

Schistosomula EVs contain CLR ligands on their surface

We next analysed the glycosylation of schistosomula EVs to assess whether ligands for CLRs were present. First, the overall N-glycan content of the EV-enriched preparations was determined by mass spectrometry (Figure 3a). MALDI-TOF mass spectra of PNGase F released N-glycans were assigned based on the detailed glycan structure descriptions available for overall N-glycan preparations of *S. mansoni* schistosomula[35]. Interestingly, the spectrum of N-glycans from the EV preparation was highly similar to previously published spectra of total extracts of three-day cultured schistosomula[24,35]. The major signals are from oligomannosidic structures of complex glycans with a core(α6)-fucose and one or two antennae consisting of Galβ1–4GlcNAc (LacNAc, LN) and/or Le^X. Structures with a core-xylose modification or GalNAcβ1–4GlcNAc (LacDiNAc or LDN) antennae with five to nine fucose residues were observed at relatively low levels (Figure 3b). These results show that schistosomula EVs contain similar N-glycans as previously found in total schistosomula extracts, including Le^X and oligomannose motifs, which are both ligands for DC-SIGN and MR[21,23].

To identify specific N-glycans that might be available for interaction with CLRs on the surface of EVs, we treated intact EVs with PNGase F to release all ('surface') N-glycans that were accessible to the enzyme. MALDI-TOF-MS analysis was performed on both the released 'surface' N-glycans as well as on the remaining N-glycans of the PNGase F-treated ('shaved') EVs (Figure 3c-d), which likely represent glycans on the inside of the EVs. Interestingly, the most

→ Figure 3. Schistosomula EV-surface N-glycans include DC-SIGN ligands

Basic scheme of the protocol for obtaining the N-glycan spectra (images adjusted from Servier Medical Art) (a), details can be found in the materials and methods. PNGase F released N-glycans measured by MALDI-TOF-MS from total (b), intact (PGNase F accessible N-glycans, 'surface') (c), and PNGase F treated (PGNase F non-accessible N-glycans on either surface or inside of the EV, 'shaved') (d) EV-enriched preparations. Signals are labelled with monoisotopic masses. Putative structural assignments were deduced from these masses based on hydrofluoric acid (HF) treatment (data not shown) and published data of schistosomula glycans[35]. Spectra shown are representative for three biological replicates. Red triangle, fucose; yellow circle, galactose; green circle, mannose; blue square, N-acetylglucosamine; yellow square, N-acetylgalactosamine; white star, xylose; *, signals corresponding to a hexose oligomer of unknown origin; #, non-glycan signals

abundantly detected N-glycans on the EV surface contained one or two Le^x antennae (Figure 3c) while the major glycans of the 'shaved' EVs were the oligomannosidic structures (Fig 3d). These results show that the glycoproteins on the surface of schistosomula EVs carry a specific subset of N-glycans with Le^x motifs, which are potential ligands for DC-SIGN or MR in the context of pathogen-host interactions[19,40,41].

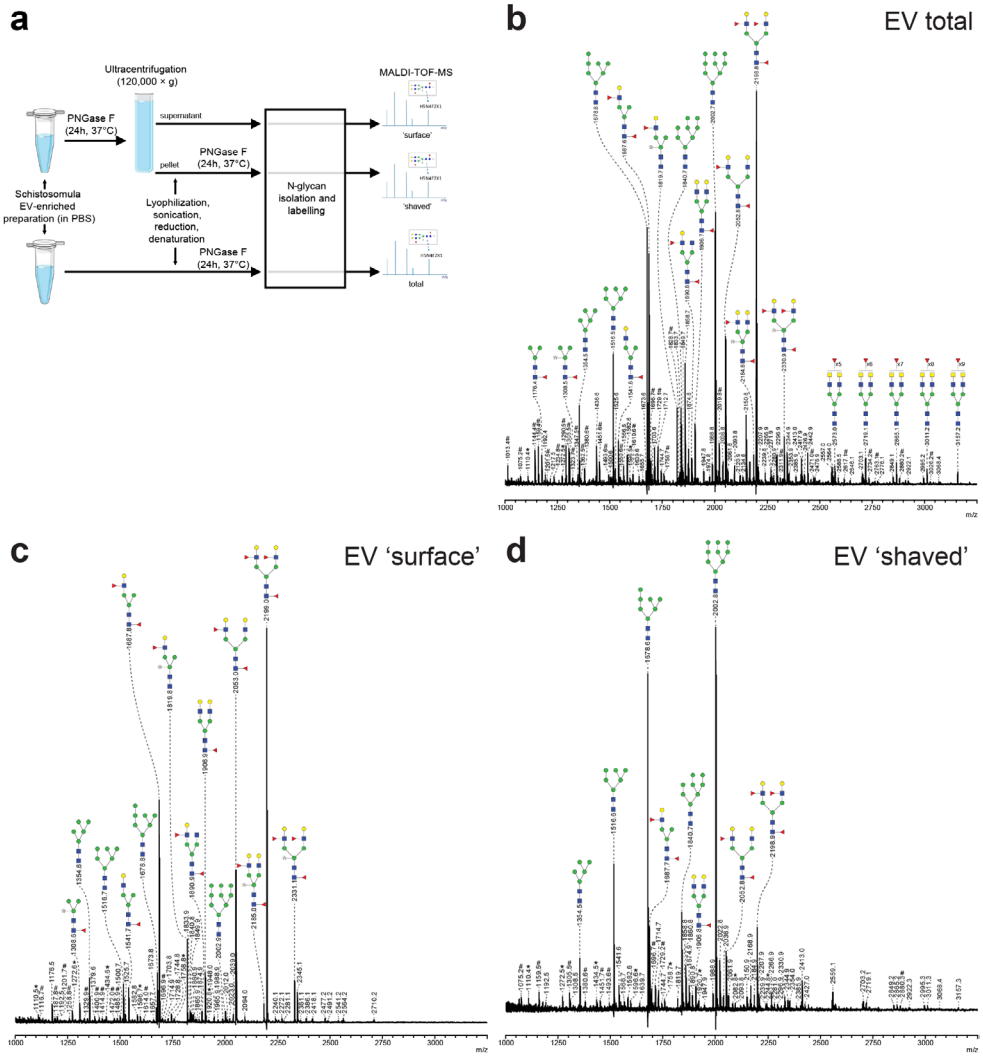

EVs are internalized via DC-SIGN but not MR or DCIR

To investigate whether DC-SIGN or MR on moDCs were involved in uptake of schistosomula EVs via glycan motifs on these EVs, moDCs were pre-incubated with antibodies blocking DC-SIGN or MR and subsequently incubated with labelled schistosomula EVs for 2 h (Figure 4a-b). In addition we investigated EV binding after blocking DCIR, a receptor expressed on moDCs that does not bind Le^x containing glycans but has been shown to bind *S. mansoni* cercarial extract[19]. Blocking DC-SIGN led to almost complete inhibition of EV uptake while blocking the MR, DCIR, or pre-incubation with the isotype control did not reduce EV internalisation. Inhibition of EV internalisation after DC-SIGN block was confirmed by confocal microscopy (Figure 4c). This reveals that schistosomula EVs were internalised by moDCs via DC-SIGN.

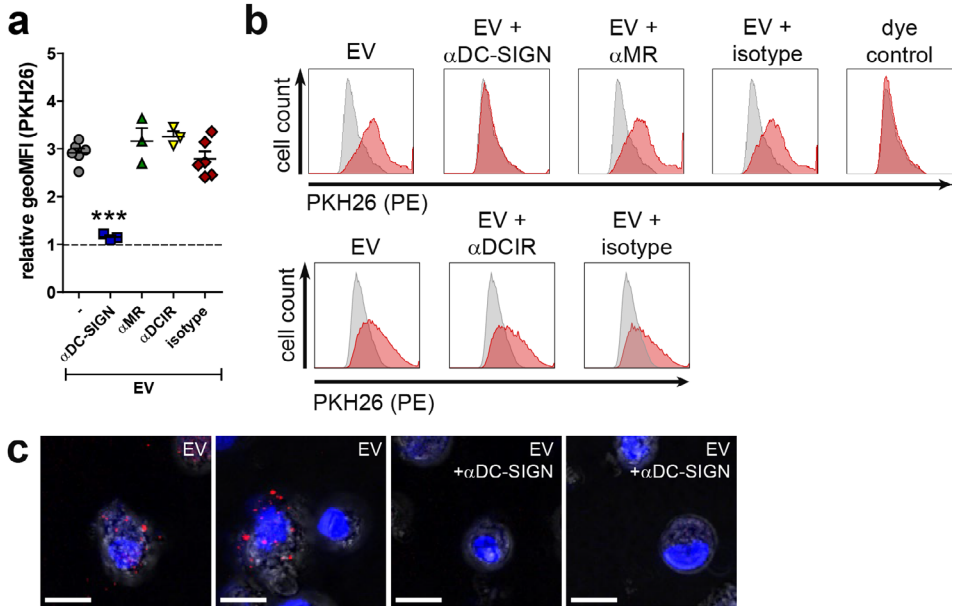

Figure 4. Schistosomula EVs are internalised via interactions with CLR DC-SIGN

PKH26 fluorescence of $CD1a^+$ cells with indicated pre-incubations (x-axis). The geoMFI (geometric mean fluorescent intensity) is shown relative to cells in medium only (a). MoDC from three to six donors. Representative histograms of two donors from same data plotted in a (b). Confocal microscopy visualisation of EV uptake and inhibition of EV uptake when DC-SIGN was blocked (c). Images show maximum projections of recorded z-stacks. PKH26-labelled EVs are stained in red and the nuclei in blue (Hoechst). Scale bar is 10 µm. Selected images are representative for three donors. Mean±SEM ***$p < 0.001$, using repeated measures ANOVA with Tukey's Multiple Comparison Test. MR, mannose receptor

EV-associated glycolipid-glycans include DC-SIGN ligands

Given that the EV surface contained DC-SIGN ligands, including the Le^x motif, we investigated whether EV deprived from surface N-glycans by PNGase F treatment would still be internalised by moDCs. Interestingly, the PNGase F-treated EVs showed a minor but not significant reduction in internalisation, and the EV uptake could still be inhibited by blocking DC-SIGN (Figure 5a). Since it has been shown that cercariae produce glycolipid-glycans that contain Le^x and other potential DC-SIGN ligands[35,42], we additionally determined the total lipid-derived glycan profile of the schistosomula EVs (Figure 5b). Here we detected a heterogeneous set of highly α3-fucosylated glycolipid structures, mostly similar to the glycolipid-glycans found in total schistosomula extract[35]. Interestingly, these lipid-glycans had terminal motifs that contained Le^x, Fucα1-3Galβ1-4(Fucα1-3) GlcNAc (pseudo-Lewis Y(Le^y)) and GalNAcβ1-4(Fucα1-3)GlcNAc (LDN-F) (Figure 5b insert), which are all previously described ligands of DC-SIGN[42,43]. These data suggest that additional to surface N-glycans, EV-associated lipid-glycans play a role in interaction with DC-SIGN.

Schistosomula EVs induced increased cytokine release and costimulatory molecule expression on moDCs

Next, we investigated whether incubation of moDCs with schistosomula EVs affect their activation status and cytokine production. We first incubated human moDCs for 24 h with EV-enriched preparations but observed no or very low release of cytokines. Therefore, in addition to EVs, moDCs were co-cultured with IL-1β and TNF-α, cytokines that are released by immune cells upon schistosome infection[3], allowing us to further investigate whether EVs could change the activation status of moDCs. Under these conditions, schistosomula EVs significantly increased IL-6, IL-10 and IL-12 secretion by moDCs (Figure 6a).

Furthermore, a significant upregulation of the costimulatory molecules CD80, CD86 and regulatory surface molecule PD-L1 was observed, while there was no significant effect on CD40, HLA-DR and PD-L2 expression (Figure 6b). These data suggest that the EV-enriched preparations were mostly synergizing or augmenting other inflammatory signals.

Role for DC-SIGN in EV-augmented immune responses

Since schistosomula-derived EVs were mainly internalised via DC-SIGN, we hypothesized that inhibiting this receptor would alter the observed augmented immune responses of moDCs by the EVs. Blocking DC-SIGN during a 24 h EV stimulation, however, did not show a significant effect on IL-6, IL-10 and IL-12 release (Figure 7a) nor on the expression of the co-stimulatory surface markers CD80,

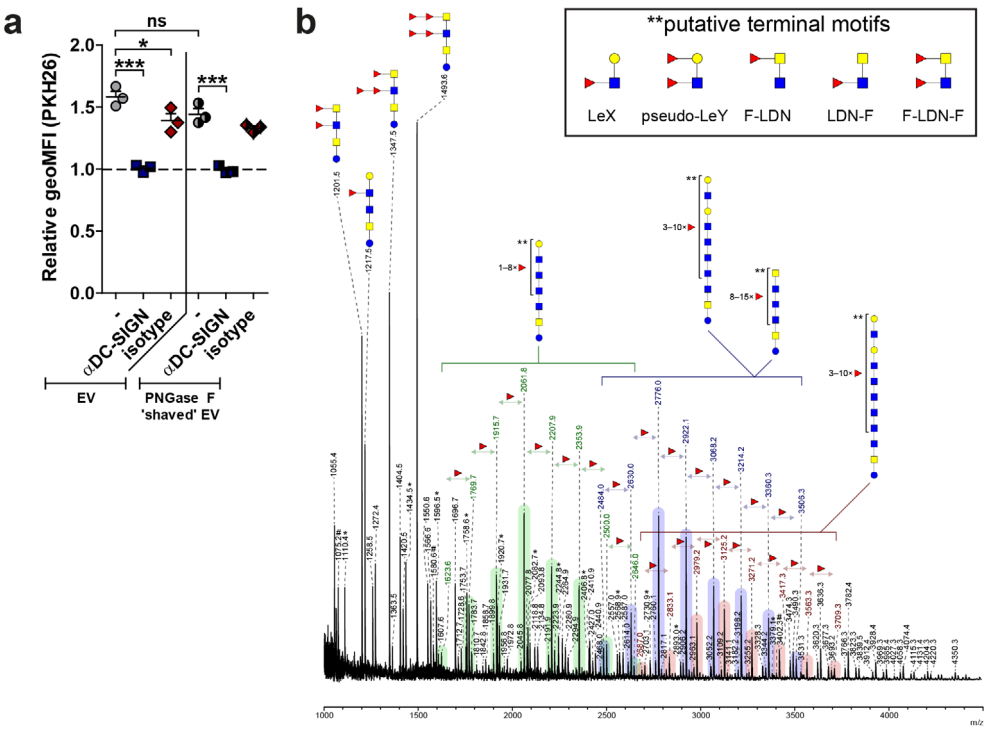

Figure 5. Internalisation of schistosomula EVs without surface N-glycans via DC-SIGN and EV-associated glycolipid-glycans

The geoMFI (geometric mean fluorescent intensity) of PKH26 relative to unstimulated moDC after 2 h incubation with labelled EVs that were treated without or with PNGase F (a). Pre-incubations are indicated on the x-axis. MoDC from 3 donors. Mean±SEM *$p < 0.05$, ***$p < 0.001$, using repeated measures ANOVA with Tukey's Multiple Comparison Test. EV-derived glycolipid-glycans measured by MALDI-TOF-MS (b). Signals are labelled with monoisotopic masses. Putative structural assignments were deduced from these masses based on published data of schistosomula glycans[35] and on hydrofluoric acid (HF) data (not shown). Coloured bars indicate the corresponding core structure with varying numbers of fucose substitutions. Putative terminal motifs formed by these fucoses are indicated in the insert. The spectrum shown is representative for three biological replicates. Red triangle, fucose; yellow circle, galactose; blue square, N-acetylglucosamine; yellow square, N-acetyl-galactosamine; Le^X, Lewis X; Le^Y, Lewis Y; F-LDN/LDN-F/F-LDN-F, fucosylated LacDiNAc *, signals corresponding to a hexose oligomer of unknown origin; #, non-glycan signals

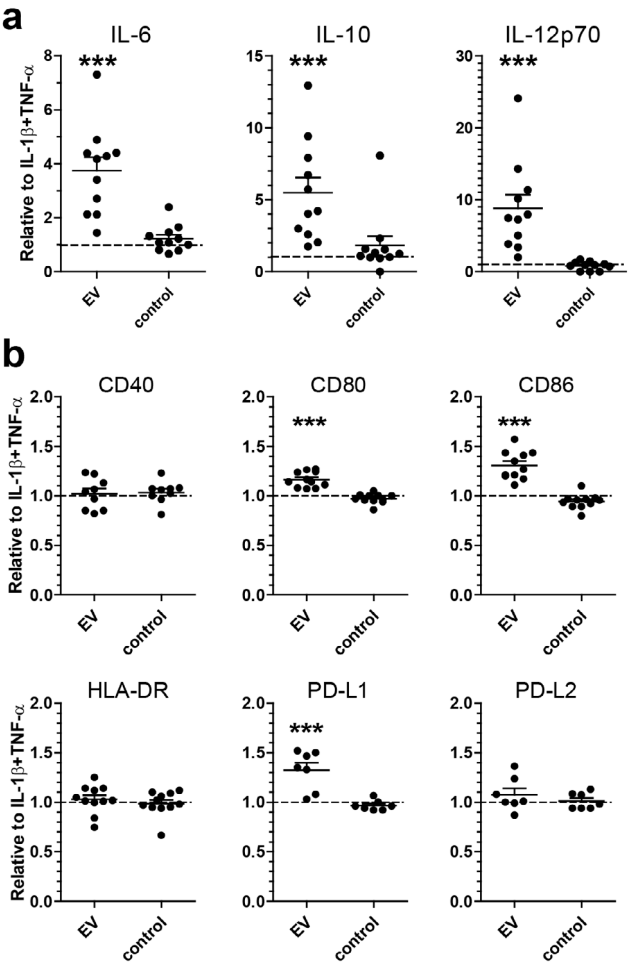

Figure 6. Schistosomula EVs augment moDC immune responses

Released cytokines (a) and surface marker expression (b) of moDC incubated with EVs. The control is medium without parasites that has been cultured and processed exactly like the schistosomula EVs. Data points are shown as fold change relative to moDC with IL-1β and TNF-α for that specific donor. MoDC from 7 to 11 donors. Mean±SEM ***p < 0.001, using repeated measures ANOVA with Dunnett's Multiple Comparison Test

CD86, HLA-DR, PD-L1 and PD-L2 after 48 h stimulation (Figure 7b). To understand why the blocking of DC-SIGN did not consistently influence the enhanced immune responses of moDCs by the EVs whereas it almost completely blocked EV internalisation after 2 h, we studied EV uptake in the presence of DC-SIGN blocking antibodies after 48 h of incubation. Blocking of DC-SIGN significantly

→ Figure 7. Role for DC-SIGN in augmented immune responses by schistosomula EVs
Released cytokines (a) and surface marker expression (b) of moDC with indicated pre-incubations (x-axes) before EV incubation. Linked points represent data from one donor. Data is shown as fold change relative to moDC with IL-1β and TNF-α from that specific donor (n=7). Summary of geometric mean fluorescent intensity (geoMFI) of moDC incubated with PKH26-labelled EVs for 48 h, relative to medium control (c) (n=6). Histograms of moDC from one representative donor from data plotted in c (d). Relative expression of mRNA from moDC after 6 h EV incubation and indicated pre-incubations (x-axes) (e) (n=5). *$p < 0.05$, ***$p < 0.001$, using repeated measures ANOVA with Tukey's Multiple Comparison Test (c) or paired student t-test (a, b, e)

reduced EV internalisation after 48 h (Figure 7c). However, the vast majority of the moDCs were still positive for the fluorescent dye, although the fluorescent intensity was lower when DC-SIGN was blocked (Figure 7d). Possibly other mechanisms than those mediated by DC-SIGN play a role in EV internalisation by moDCs after prolonged exposure. To investigate whether blocking of DC-SIGN does interfere with moDC function during shorter incubations with schistosomula-derived EVs, moDCs were stimulated with EVs in the absence or presence of blocking antibodies for 6 h, after which cytokine mRNA expression was determined. Indeed, at this time point, the effect of blocking DC-SIGN was more prominent with a significant reduction in TNF-α mRNA and a trend for lower IL-10 mRNA expression (Figure 7e). IL-12p35 mRNA levels were also reduced in most donors, though not significant. These results show that, within the first hours of exposure but not at a longer timescale, the moDC immune profile is influenced by schistosomula EVs through internalisation via DC-SIGN.

6

Discussion

Schistosome parasites are master regulators of host immune responses and they release various molecules and products to achieve this. Here we demonstrate that *S. mansoni* schistosomula release EVs that contain Le^X antigens on their surface. Interaction of the glycosylated EVs with DC-SIGN on moDCs lead to internalisation and enhanced expression of both immunostimulatory and regulatory effector molecules. Thus, schistosome EVs appear to contribute to immune modulation by the parasite.

Schistosomula are multicellular organisms, having various organs and cells as potential sources of their released EVs. It has been shown that micron-sized vesicles are released from their acetabular glands[11,44] and it is suggested that EVs can also derive from the tegument[6]. Since multicellular organisms release

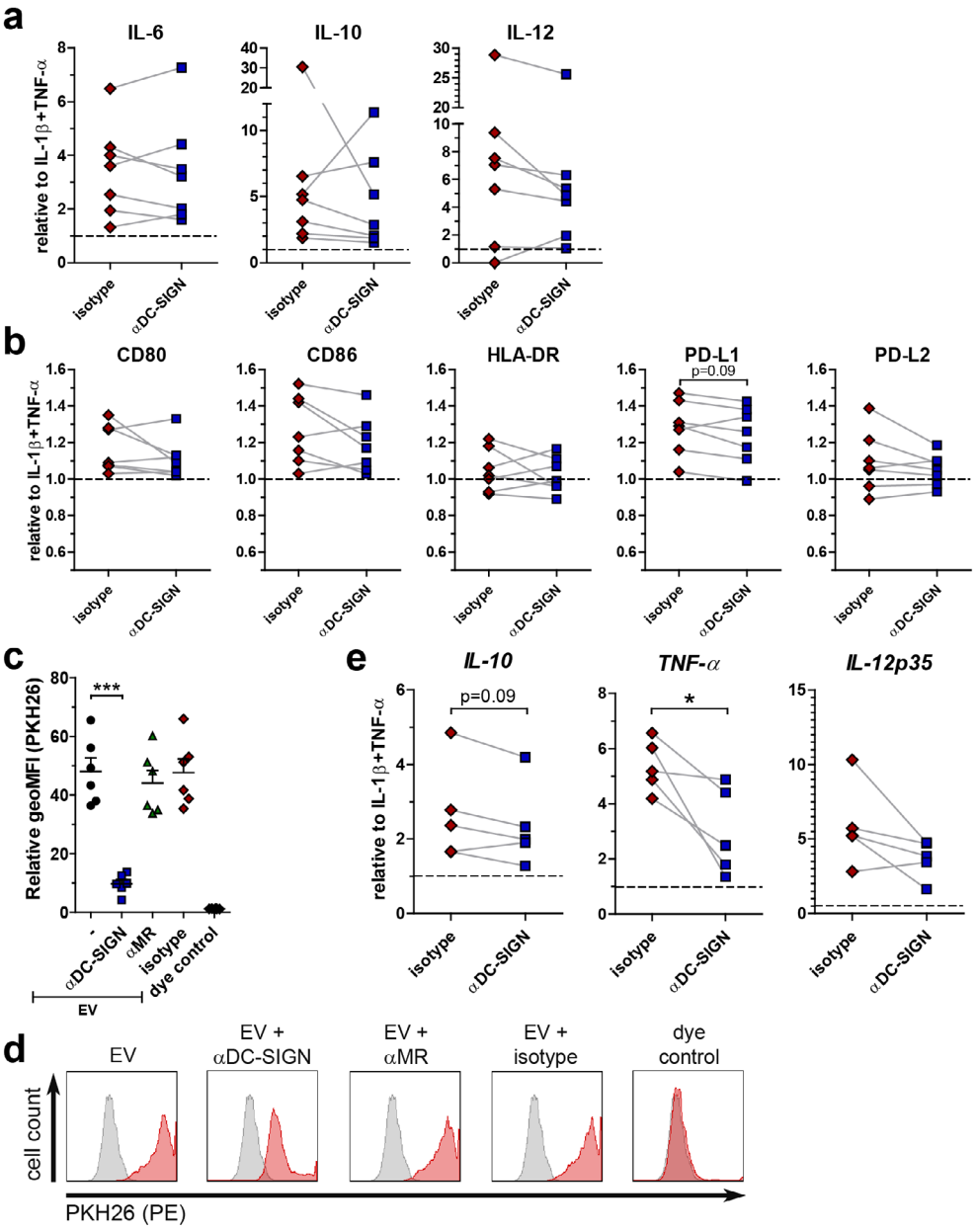

heterogeneous populations of EVs, it is likely that the moDCs can internalise these EVs via various receptors and/or routes[13]. The schistosomula-derived EV populations described here were heterogeneous in size, which we analysed with NTA (Figure 1c) and cryo EM (Figure 1e). The size of EVs may influence uptake

routes, as has been shown for *Helicobacter pylori* outer membrane vesicles (OMVs): small OMVs were taken up via caveolin-mediated endocytosis and bigger OMVs via micropinocytosis and endocytosis[45]. The major population of EVs >300 nm we observed have not been described before for *S. mansoni* schistosomula[6]. Although we used a similar schistosomula EV isolation protocol as Nowacki *et al*[6], the isolated EVs in that paper were only visualised by TEM of negatively stained EVs and not by NTA. With this same technique, our isolated schistosomula EVs also showed similar sizes <200 nm (Figure 1a-b) but only with the NTA and cryo EM the EV population >300 nm was detectable. EVs >300 nm have not been found among adult worms EVs[7,8,46]. Schistosomes are organisms with a complex life cycle and the schistosomula and adult worm life stages differ in size, shape, molecular, and cellular make up, and interaction with the host and its immune system[2,47]. Therefore, it is likely that different life stages of the parasite produce different EV populations regarding molecular content[6,48] as well as size. Furthermore, the adult worm EVs published have been isolated by different protocols which may further explain differences between the observed sizes of EVs derived from various schistosome different life stages.

Interestingly, our cryo EM data showed that around half of the schistosomula-derived EVs were covered with thin filament-like structures (Figure 1d). These structures have not been described for eukaryotic EVs so far. It remains to be explored what the molecular composition of these EV-associated structures is and whether these structures are specific for *S. mansoni* and/or specifically related to the schistosomula life stage. These thin filaments resemble the electron-dense surface layer of extracellular proteins and LPS or glycocalyx on some bacteria[49,50] and their released OMVs[51]. We hypothesize that the structures on schistosomula EVs are composed of large, complex glycoconjugates and/or include proteins with attached glycan polymers, similar to the mammalian glycocalyx consisting of proteoglycans with attached glycosaminoglycans[25]. Altogether, the EM analyses emphasize that cryo EM provides improved visualisation of the near native state of isolated EVs compared to TEM of negatively stained EVs.

EVs released by *S. mansoni* schistosomula were internalised by human moDCs (Figure 2). Previous studies have demonstrated that *S. japonicum* EVs derived from adult worms and eggs are also internalised by host cells[46,52–54]. This indicates, together with our data, that at least three lifecycle stages of *Schistosoma* in humans release EVs that interact with the host. By chelating extracellular calcium with EGTA, schistosomula EV could not bind to or be taken up by the moDC (Figure 2d-e). This suggests that the interaction of the EVs with the moDC was via the ligation of glycoconjugates to CLRs, which is calcium dependent, and not via protein-protein interaction. By inhibiting specific CLRs we show that

internalisation of schistosomula EVs by moDCs is primarily facilitated by DC-SIGN (Figure 4). This CLR is known to bind schistosome egg[21], cercarial[43], and worm antigens[55], via glycan motifs including mannotriose, Le^X, LDN-F, and pseudo-Le^Y [19,42,43]. In contrast, CLR DCIR mainly binds Le^B (Lewis B) and sulpho-Le^A (Lewis A) motifs[19], and indeed, blocking this receptor did not reduce EV uptake by the moDC. Previously, it was shown that the egg-derived glycoprotein omega-1, which carries Le^X containing N-glycans highly similar to those found here on the EVs (Figure 3), is mainly internalised by moDCs via the MR[22]. However, when blocking the MR, EV internalisation was not inhibited. This difference of internalisation routes between omega-1 and EVs could be explained by the characteristics of the two CLRs: DC-SIGN has one carbohydrate recognition domain (CRD), is present as tetramers, and it clusters in (lipid raft) nanodomains that are distributed on the cell membrane. Clustering increases the avidity of low affinity glycan-lectin interactions and allows this receptor to interact at multiple sites with pathogens that differ greatly in size[56]. On the other hand, the MR consists of multiple CRDs, which results in binding of multivalent or repetitive ligands to a single MR monomer[57]. Considering these aspects, larger particles such as EVs would favour DC-SIGN mediated uptake while smaller glycosylated proteins are more likely to be internalised via other receptors, such as the MR. A very recent publication substantiates this theory by showing that tumour-derived apoptotic EVs with high-mannose glycans on their surface were mainly internalized via interaction with DC-SIGN and not the MR[58]. Furthermore, it suggests that, together with our findings, DC-SIGN mediated EV uptake may be a widely occurring mechanism, across a broad spectrum of species and may not be exclusive to schistosomula-derived EVs. Of note is that helminths, including *S. mansoni*, lack sialic acid in their glycan repertoire, which is a fundamental difference with mammalian glycans. It was recently found that EVs released by human glioblastoma cells had complex sialic acid-capped N-glycans on their surface that mainly bound to Siglec-9 on moDCs[59]. When sialic acids on the EV surface were enzymatically removed and Le^Y was inserted, EV uptake by moDC and binding of the EVs to DC-SIGN were increased. Furthermore, EVs from murine hepatic cell lines expose sialyl-Le^X on the EV surface and removing the sialic acids with neuraminidase significantly increased EV uptake by M1 cell lines[28]. However, no DC-SIGN blocking experiments were performed in these studies. Thus, the question remains whether EV internalisation via DC-SIGN is specific for schistosomula EVs, or whether it is a more general mechanism via which EVs from both pathogens and mammalian cells are internalized. However, we cannot exclude the possibility that internalisation of schistosomula EVs may be facilitated via different CLRs in a different host. For example, the murine macrophage galactose-type lectin (MGL-1)[60] can bind to Le^X

while the human MGL cannot[61]. Human MGL binds to LDN motifs, which were absent in our schistosomula EV glycan analyses.

So far, most research on glycosylation of pathogen-derived EVs focussed on lipopolysaccharides of bacterial OMVs[62–65]. Only very recently, the presence of glycoconjugates on the surface of EVs released by the helminth *Fasciola hepatica* was studied using lectin microarrays[66]. Here we performed a more detailed structural analysis of glycans associated with EVs released by a helminth parasite. Using mass spectrometry we showed the presence of mainly complex type N-glycans with Le^x motifs as well as oligomannose and high mannose glycans (Figure 3b) and the presence of lipid-linked glycans with Le^x, pseudo-Le^y, and other α3-fucosylated glycan motifs (Figure 5b). The EV N-glycan profile was qualitatively very similar to that of whole schistosomula[35]. The overall glycosylation pattern associated with this particular schistosome life stage was reflected in the EVs, however, with differences in relative abundances of the glycans. Biological replicates of the parasite culture and EV isolation generated at two different laboratories (Leiden and Aberystwyth) showed similar N-glycan profiles, confirming the reproducibility of the EV isolation protocol and glycan patterns[6]. Mostly complex glycans with Le^x motifs were cleaved from intact EVs by incubation with PNGase-F (Figure 3c), implicating that these structures were on the EV surface. Glycoconjugates on the EV surface can influence their cellular internalisation, as was shown for bacterial OMV[65], murine hepatic cell line EVs[28], tumour-derived EVs[58,59], and *F. hepatica* adult worm EVs[66]. Interestingly, PNGase F treated EVs were still internalised by moDC via DC-SIGN (Figure 5a). This indicates that other glycans with DC-SIGN ligands such as the fucosylated lipid-linked glycans play a role in this process, either specifically or in addition to the N-glycans. Mass spectrometry analysis showed the presence of EV-associated glycolipid-glycans (Figure 5b) containing several structures that were reported previously for schistosomula[35], but with more extended higher molecular weight structures. Our data indicate that many of the EV lipid-derived glycans contain motifs such as Le^x, pseudo-Le^y, and other α3-linked fucose containing motifs that can bind to DC-SIGN[42,43], which may explain why PNGase-F treated EVs could still be internalised via DC-SIGN. Furthermore, *S. mansoni* produce various O-glycans[35], which are possibly also present on EVs and contribute to EV-CLR interaction. We therefore suggest that both N-glycans and glycolipid-glycans, and possibly O-glycans, contribute to the interaction of the EVs with DC-SIGN. This interaction is most likely via Le^x motifs, which are abundant in these glycan types, with the possible contribution of other α3-fucosylated lipid-glycans.

Interestingly, the complex type N-glycans on the EV surface and many of the glycolipids of the schistosmula EVs contain antigenic glycan motifs that

were previously shown to be the target of antibodies of various isotypes during schistosome infection. These motifs include N-glycan core-xylose, Le^x, and the various fucosylated glycolipid motifs[67–69]. It is therefore tempting to speculate that EVs can either elicit these antibodies and/or that EVs are targeted by antibodies generated against other, similarly glycosylated, antigens produced by schistosomes during an infection. Antibodies that recognize and bind molecules on the EV surface can facilitate internalisation by APCs, for example via Fc receptors. Antibody-bound EVs can be targeted to different intracellular compartments compared to EVs without antibodies. This has been observed for EVs from the helminth *Heligmosomoides polygyrus*[70]. *H. polygyrus* EVs pre-incubated with antisera were targeted to lysosomes. However, lysosome targeting has also been observed for antigens internalised by DC-SIGN[71]. Another possibility is that EV uptake is enhanced after incubation with antisera, which was observed for *F. hepatica* EVs and RAW264.7 macrophages[66]. Differences in route of uptake can possibly alter the fate of the EVs and thus possibly influence EV-induced immunomodulation.

Cross-species communication via EVs that contributes to modulation of host immune responses has been described previously for helminths, including *H. polygyrus*[70] and *Nippostrongylus brasiliensis*[72]. In this study, we observed that *S. mansoni* schistosomula EVs are capable of augmenting activation-induced cytokine secretion and surface molecule expression by human moDCs, including both immunostimulatory and regulatory factors (Figure 6). It has been suggested that a delicate balance between benefit for the host and benefit for the parasite contributes to overall survival of the parasite within the host with limited pathology[3]. The induction of pro-inflammatory cytokines is a natural response of the host to the skin-invading pathogen, however, this response is transient. Priming of a protective adaptive immune response is hampered, probably via the induction of regulatory responses by the parasite, such as increased IL-10 release and PD-L1 expression[12], allowing the parasite to develop into mature worms and start egg laying. Different molecules present in the heterogenous EV population may have contributed to the observed augmented immune responses. It is known that DC-SIGN signalling via fucose ligands, which are motifs found on the N-glycan and lipid-glycan structures of the EVs, mainly increases IL-10 and decreases pro-inflammatory responses[73]. In contrast, we observed that blocking DC-SIGN actually decreased pro-inflammatory TNF-α and IL-12 mRNA and did not fully reduce the responses to baseline (Figure 7e). Thus, it is likely to assume that schistosomula EVs contain a mix of various (glycosylated) proteins and RNAs (amongst other biological molecules, such as lipids[74]) that all may contribute to a combined effect on host immunity[6]. Indeed, the NTA data as well as the cryo EM show at least a variation in EV size and with or without the thin filaments,

and it is tempting to speculate that these different EVs may show variation in their surface glycan profile and may have specific activities on host immunity. Interestingly, since total ES from schistosomula increases IL-12, IL-6 and IL-10 release as well as CD86 expression by mouse BMDCs[11], it is tempting to suggest that part of the effects of the ES are mediated by the EVs in that secretion.

In contrast to the strong blocking effect of anti-DC-SIGN antibodies on EV internalisation (Figure 4 and Figure 7c), however, blocking DC-SIGN did not significantly alter EV-augmented immune responses during prolonged stimulation (Figure 7a-b). The variation we detected among donors in reduction or increase of IL-10 release in the presence of blocking DC-SIGN (Figure 7a) was also observed in another study that examined glycan-mediated effects by larval ES[75]. These donor-specific variances could be associated with intrinsic DC-SIGN levels, which vary highly between and within donors[76]. Furthermore, residual uptake of EVs via other processes such as (macro-)pinocytosis or protein-protein interaction could still have affected the immune activation of moDCs upon prolonged culture (Figure 7d). Shorter incubation, however, showed that part of the augmented immune profile of moDCs by schistosomula EVs was indeed dependent on interaction with DC-SIGN (Figure 7e) and provides evidence that interaction of glycans on the EV surface with DC-SIGN does play a role in immune modulation of host responses.

In conclusion, our study demonstrates that *S. mansoni* schistosomula release glycosylated EVs that carry Le^X, pseudo-Le^Y, and other fucosylated motifs, and we reveal a distinct role for DC-SIGN in glycan-mediated internalisation of EVs by host immune cells. This interaction contributes to increased pro- and anti-inflammatory responses, substantiating that EVs play a role in host immune regulation by helminths to establish and control infection. Future studies on how EV-associated molecules contribute to immune modulation will further our understanding of parasite-host interactions and may provide insights for vaccine development.

6

Authors' contributions

M.E.K. contributed to conceiving the study, performed the schistosomula cultures, EV isolations, NTA, cryo EM measurements, moDC isolations/stimulations, ELISAs, flow cytometry, RNA extraction, qPCR, data analysis, and drafting of the manuscript. A.J.H. assisted with moDC isolations/differentiation and constructing flow cytometry panels. A.O.F. performed shedding of snails to obtain cercariae and assisted with moDC isolations. D.L.N. performed the N-glycan characterization and assisted with the analysis of the spectra. C.M.K. performed the confocal microscopy and generated the confocal images. R.I.K. performed the cryo EM imaging and assisted with the subsequent analysis. J.J.T. performed the TEM

imaging and contributed to the TEM analysis. K.F.H. contributed to the design of experiments, interpretation of the results and correcting the manuscript. E.N.-'tH. contributed to conceiving the study, the design of the experiments, overseeing the EV isolation, interpretation of the results and drafting of the manuscript. H.H.S. and C.H.H. both participated in conceiving the study, the design of the experiments, interpretation of the results and drafting of the manuscript. All authors read and approved the final manuscript.

Acknowledgements

We would like to thank Jan de Best, Frank Otto and the rest of the *S. mansoni* life-cycle team for maintaining the availability of *S. mansoni* parasites, Pieter Vader from the University Medical Center Utrecht (The Netherlands) for using the NanoSight, Thiago Patente, Anna Zawistowska-Deniziak, Leonard Pelgrom, Roos van Schuijlenburg, Nikolas Duszenko, and Eline Brombacher for assisting with cell isolation/differentiation and feedback on the moDC model, the staff from the LUMC Flow Cytometry Core Facility for maintaining the flow cytometer used, Fanny Nowacki for providing EVs from Aberystwyth, Mr Alan Cookson of the Aberystwyth University Advanced Microscopy and Bio-imaging Laboratory for his help and support with TEM, Lisa Koorneef, Bruno Guigas, and Tom Driedonks for discussing qPCR analysis, and Koen Stam for feedback on the statistical analysis.

Disclosure of interest

The authors report no conflict of interest.

Funding

This work was supported by grants from NWO Graduate School Program 022.006.010 (to M.E.K.); ZonMW-Vidi 20972 (to H.H.S.); the European Research Council under the European Union's Seventh Framework Programme [FP/2007–2013]/ERC Grant Agreement No. 337581 (to E.N.-'tH.).

References

1. Colley, D. G., Bustinduy, A. L., Secor, W. E. & King, C. H. Human schistosomiasis. *The Lancet* **383**, 2253–2264 (2014).
2. Maizels, R. M., Smits, H. H. & McSorley, H. J. Modulation of Host Immunity by Helminths: The Expanding Repertoire of Parasite Effector Molecules. *Immunity* **49**, 801–818 (2018).
3. Mountford, A. P. & Trottein, F. Schistosomes in the skin: a balance between immune priming and regulation. *Trends Parasitol* **20**, 221–226 (2004).
4. Maizels, R. M. & McSorley, H. J. Regulation of the host immune system by helminth parasites. *Journal of Allergy and Clinical Immunology* **138**, 666–675 (2016).
5. Wu, Z. *et al.* Extracellular Vesicle-Mediated Communication Within Host-Parasite Interactions. *Front Immunol* **9**, 3066 (2018).
6. Nowacki, F. C. *et al.* Protein and small non-coding RNA-enriched extracellular vesicles are released by the pathogenic blood fluke Schistosoma mansoni. *J Extracell Vesicles* **4**, 28665 (2015).
7. Sotillo, J. *et al.* Extracellular vesicles secreted by Schistosoma mansoni contain protein vaccine candidates. *Int J Parasitol* **46**, 1–5 (2016).
8. Samoil, V. *et al.* Vesicle-based secretion in schistosomes: Analysis of protein and microRNA (miRNA) content of exosome-like vesicles derived from Schistosoma mansoni. *Sci Rep* **8**, 3286 (2018).
9. Maizels, R. M. & Yazdanbakhsh, M. Immune Regulation by helminth parasites: cellular and molecular mechanisms. *Nature Reviews Immunology* **3**, 733–744 (2003).
10. Hogg, K. G., Kumkate, S., Anderson, S. & Mountford, A. P. Interleukin-12 p40 secretion by cutaneous CD11c+ and F4/80+ cells is a major feature of the innate immune response in mice that develop Th1-mediated protective immunity to Schistosoma mansoni. *Infect Immun* **71**, 3563–3571 (2003).
11. Paveley, R. A., Aynsley, S. A., Cook, P. C., Turner, J. D. & Mountford, A. P. Fluorescent imaging of antigen released by a skin-invading helminth reveals differential uptake and activation profiles by antigen presenting cells. *PLoS Negl Trop Dis* **3**, e528 (2009).
12. Winkel, B. M. F. *et al.* Early Induction of Human Regulatory Dermal Antigen Presenting Cells by Skin-Penetrating Schistosoma Mansoni Cercariae. *Front Immunol* **9**, 2510 (2018).
13. van Niel, G., D'Angelo, G. & Raposo, G. Shedding light on the cell biology of extracellular vesicles. *Nat Rev Mol Cell Biol* **19**, 213–228 (2018).
14. Egesa, M. *et al.* Schistosoma mansoni schistosomula antigens induce Th1/Pro-inflammatory cytokine responses. *Parasite Immunol* **40**, e12592 (2018).
15. Jenkins, S. J., Hewitson, J. P., Ferret-Bernard, S. & Mountford, A. P. Schistosome larvae stimulate macrophage cytokine production through TLR4-dependent and -independent pathways. *Int Immunol* **17**, 1409–1418 (2005).
16. Paveley, R. A. *et al.* The Mannose Receptor (CD206) is an important pattern recognition receptor (PRR) in the detection of the infective stage of the helminth Schistosoma mansoni and modulates IFNgamma production. *Int J Parasitol* **41**, 1335–1345 (2011).
17. van Die, I. & Cummings, R. D. The Mannose Receptor in Regulation of Helminth-Mediated Host Immunity. *Front Immunol* **8**, 1677 (2017).

18. Kaisar, M. M. M. *et al.* Dectin-1/2-induced autocrine PGE2 signaling licenses dendritic cells to prime Th2 responses. *PLoS Biol* **16**, e2005504 (2018).
19. Bloem, K. *et al.* DCIR interacts with ligands from both endogenous and pathogenic origin. *Immunol Lett* **158**, 33–41 (2014).
20. van Liempt, E. *et al.* Schistosoma mansoni soluble egg antigens are internalized by human dendritic cells through multiple C-type lectins and suppress TLR-induced dendritic cell activation. *Mol Immunol* **44**, 2605–2615 (2007).
21. van Die, I. *et al.* The dendritic cell-specific C-type lectin DC-SIGN is a receptor for Schistosoma mansoni egg antigens and recognizes the glycan antigen Lewis x. *Glycobiology* **13**, 471–478 (2003).
22. Everts, B. *et al.* Schistosome-derived omega-1 drives Th2 polarization by suppressing protein synthesis following internalization by the mannose receptor. *J Exp Med* **209**, 1753–67, S1 (2012).
23. Geijtenbeek, T. B. & Gringhuis, S. I. C-type lectin receptors in the control of T helper cell differentiation. *Nat Rev Immunol* **16**, 433–448 (2016).
24. Jang-Lee, J. *et al.* Glycomics analysis of Schistosoma mansoni egg and cercarial secretions. *Mol Cell Proteomics* **6**, 1485–1499 (2007).
25. Gerlach, J. Q. & Griffin, M. D. Getting to know the extracellular vesicle glycome. *Mol Biosyst* **12**, 1071–1081 (2016).
26. Williams, C. *et al.* Glycosylation of extracellular vesicles: current knowledge, tools and clinical perspectives. *J Extracell Vesicles* **7**, 1442985 (2018).
27. Freitas, D. *et al.* Different isolation approaches lead to diverse glycosylated extracellular vesicle populations. *J Extracell Vesicles* **8**, (2019).
28. Williams, C. *et al.* Assessing the role of surface glycans of extracellular vesicles on cellular uptake. *Scientific Reports* **9**, (2019).
29. Shimoda, A., Sawada, S., Sasaki, Y. & Akiyoshi, K. Exosome surface glycans reflect osteogenic differentiation of mesenchymal stem cells: Profiling by an evanescent field fluorescence-assisted lectin array system. *Scientific Reports* **9**, (2019).
30. Colley, D. G. & Wikel, S. K. Schistosoma mansoni: simplified method for the production of schistosomules. *Exp Parasitol* **35**, 44–51 (1974).
31. Van Deun, J. *et al.* EV-TRACK: transparent reporting and centralizing knowledge in extracellular vesicle research. *Nat Methods* **14**, 228–232 (2017).
32. Schindelin, J. *et al.* Fiji: an open-source platform for biological-image analysis. *Nat Methods* **9**, 676–682 (2012).
33. Hussaarts, L. *et al.* Rapamycin and omega-1: mTOR-dependent and -independent Th2 skewing by human dendritic cells. *Immunol Cell Biol* **91**, 486–489 (2013).
34. Wilbers, R. H. P. *et al.* Production and glyco-engineering of immunomodulatory helminth glycoproteins in plants. *Scientific Reports* **7**, (2017).
35. Smit, C. H. *et al.* Glycomic Analysis of Life Stages of the Human Parasite Schistosoma mansoni Reveals Developmental Expression Profiles of Functional and Antigenic Glycan Motifs. *Mol Cell Proteomics* **14**, 1750–1769 (2015).

36. Ceroni, A. *et al.* GlycoWorkbench: a tool for the computer-assisted annotation of mass spectra of glycans. *J Proteome Res* **7**, 1650–1659 (2008).
37. Bustin, S. A. *et al.* The MIQE guidelines: minimum information for publication of quantitative real-time PCR experiments. *Clin Chem* **55**, 611–622 (2009).
38. Simonsen, J. B. Pitfalls associated with lipophilic fluorophore staining of extracellular vesicles for uptake studies. *J Extracell Vesicles* **8**, 1582237 (2019).
39. Hokke, C. H. & van Diepen, A. Helminth glycomics - glycan repertoires and host-parasite interactions. *Mol Biochem Parasitol* **215**, 47–57 (2017).
40. van Kooyk, Y. & Geijtenbeek, T. B. DC-SIGN: escape mechanism for pathogens. *Nat Rev Immunol* **3**, 697–709 (2003).
41. Everts, B. *et al.* Omega-1, a glycoprotein secreted by Schistosoma mansoni eggs, drives Th2 responses. *J Exp Med* **206**, 1673–1680 (2009).
42. Meevissen, M. H. J. *et al.* Specific glycan elements determine differential binding of individual egg glycoproteins of the human parasite Schistosoma mansoni by host C-type lectin receptors. *Int J Parasitol* **42**, 269–277 (2012).
43. Meyer, S. *et al.* DC-SIGN mediates binding of dendritic cells to authentic pseudo-LewisY glycolipids of Schistosoma mansoni cercariae, the first parasite-specific ligand of DC-SIGN. *J Biol Chem* **280**, 37349–37359 (2005).
44. Dorsey, C. H., Cousin, C. E., Lewis, F. A. & Stirewalt, M. A. Ultrastructure of the Schistosoma mansoni cercaria. *Micron* **33**, 279–323 (2002).
45. Turner, L. *et al.* Helicobacter pylori Outer Membrane Vesicle Size Determines Their Mechanisms of Host Cell Entry and Protein Content. *Front Immunol* **9**, 1466 (2018).
46. Liu, J. *et al.* Schistosoma japonicum extracellular vesicle miRNA cargo regulates host macrophage functions facilitating parasitism. *PLoS Pathog* **15**, e1007817 (2019).
47. Dunne, D. W. & Cooke, A. Opinion - A worm's eye view of the immune system: consequences for evolution of human autoimmune disease. *Nature Reviews Immunology* **5**, 420–426 (2005).
48. Kifle, D. W. *et al.* Proteomic analysis of two populations of Schistosoma mansoni-derived extracellular vesicles: 15k pellet and 120k pellet vesicles. *Mol Biochem Parasitol* **236**, 111264 (2020).
49. Hunter, R. C. & Beveridge, T. J. High-resolution visualization of Pseudomonas aeruginosa PAO1 biofilms by freeze-substitution transmission electron microscopy. *J Bacteriol* **187**, 7619–7630 (2005).
50. Liu, Y., Hidaka, E., Kaneko, Y., Akamatsu, T. & Ota, H. Ultrastructure of Helicobacter pylori in human gastric mucosa and H. pylori-infected human gastric mucosa using transmission electron microscopy and the high-pressure freezing-freeze substitution technique. *J Gastroenterol* **41**, 569–574 (2006).
51. Gui, M. J., Dashper, S. G., Slakeski, N., Chen, Y. Y. & Reynolds, E. C. Spheres of influence:Porphyromonas gingivalisouter membrane vesicles. *Molecular Oral Microbiology* **31**, 365–378 (2016).
52. Wang, L. *et al.* Exosome-like vesicles derived by Schistosoma japonicum adult worms mediates M1 type immune- activity of macrophage. *Parasitol Res* 114, 1865–1873 (2015).
53. Zhu, L. *et al.* Molecular characterization of S. japonicum exosome-like vesicles reveals their regulatory roles in parasite-host interactions. *Sci Rep* 6, 25885 (2016).

54. Zhu, S. *et al.* Release of extracellular vesicles containing small RNAs from the eggs of Schistosoma japonicum. *Parasit Vectors* 9, 574 (2016).
55. van Stijn, C. M. *et al.* Schistosoma mansoni worm glycolipids induce an inflammatory phenotype in human dendritic cells by cooperation of TLR4 and DC-SIGN. *Mol Immunol* **47**, 1544–1552 (2010).
56. Garcia-Vallejo, J. J. & van Kooyk, Y. The physiological role of DC-SIGN: a tale of mice and men. *Trends Immunol* **34**, 482–486 (2013).
57. Gazi, U. & Martinez-Pomares, L. Influence of the mannose receptor in host immune responses. *Immunobiology* **214**, 554–561 (2009).
58. Horrevorts, S. K. *et al.* Glycan-Modified Melanoma-Derived Apoptotic Extracellular Vesicles as Antigen Source for Anti-Tumor Vaccination. *Cancers (Basel)* **11**, (2019).
59. Dusoswa, S. A. *et al.* Glycan modification of glioblastoma-derived extracellular vesicles enhances receptor-mediated targeting of dendritic cells. *J Extracell Vesicles* **8**, 1648995 (2019).
60. Eriksson, M. *et al.* Biological evaluation of multivalent lewis X-MGL-1 interactions. *Chembiochem* **15**, 844–851 (2014).
61. Marcelo, F. *et al.* Identification of a secondary binding site in human macrophage galactose-type lectin by microarray studies: Implications for the molecular recognition of its ligands. *Journal of Biological Chemistry* **294**, 1300–1311 (2019).
62. Kaparakis, M. *et al.* Bacterial membrane vesicles deliver peptidoglycan to NOD1 in epithelial cells. *Cell Microbiol* **12**, 372–385 (2010).
63. Stevenson, T. C. *et al.* Immunization with outer membrane vesicles displaying conserved surface polysaccharide antigen elicits broadly antimicrobial antibodies. *Proc Natl Acad Sci U S A* **115**, E3106–E3115 (2018).
64. Kuipers, M. E., Hokke, C. H., Smits, H. H. & Hoene, E. N. M. N. '. Pathogen-Derived Extracellular Vesicle-Associated Molecules That Affect the Host Immune System: An Overview. *Frontiers in Microbiology* **9**, 2182 (2018).
65. O'Donoghue, E. J. *et al.* Lipopolysaccharide structure impacts the entry kinetics of bacterial outer membrane vesicles into host cells. *PLoS Pathog* **13**, e1006760 (2017).
66. de la Torre-Escudero, E. *et al.* Surface molecules of extracellular vesicles secreted by the helminth pathogen Fasciola hepatica direct their internalisation by host cells. *PLoS Negl Trop Dis* **13**, e0007087 (2019).
67. Nkurunungi, G. *et al.* Microarray assessment of N-glycan-specific IgE and IgG profiles associated with Schistosoma mansoni infection in rural and urban Uganda. *Sci Rep* **9**, 3522 (2019).
68. van Diepen, A. *et al.* Differential anti-glycan antibody responses in Schistosoma mansoni-infected children and adults studied by shotgun glycan microarray. *PLoS Negl Trop Dis* **6**, e1922 (2012).
69. Yang, Y. Y. *et al.* Specific anti-glycan antibodies are sustained during and after parasite clearance in Schistosoma japonicum-infected rhesus macaques. *PLoS Negl Trop Dis* **11**, e0005339 (2017).
70. Coakley, G. *et al.* Extracellular Vesicles from a Helminth Parasite Suppress Macrophage Activation and Constitute an Effective Vaccine for Protective Immunity. *Cell Rep* **19**, 1545–1557 (2017).

71. Engering, A. *et al.* The dendritic cell-specific adhesion receptor DC-SIGN internalizes antigen for presentation to T cells. *J Immunol* **168**, 2118–2126 (2002).
72. Eichenberger, R. M. *et al.* Hookworm Secreted Extracellular Vesicles Interact With Host Cells and Prevent Inducible Colitis in Mice. *Front Immunol* **9**, 850 (2018).
73. Gringhuis, S. I., Kaptein, T. M., Wevers, B. A., Mesman, A. W. & Geijtenbeek, T. B. Fucose-specific DC-SIGN signalling directs T helper cell type-2 responses via IKKepsilon- and CYLD-dependent Bcl3 activation. *Nat Commun* **5**, 3898 (2014).
74. Giera, M. *et al.* The Schistosoma mansoni lipidome: Leads for immunomodulation. *Analytica Chimica Acta* **1037**, 107–118 (2018).
75. Turner, J. D. *et al.* Schistosome infection is associated with enhanced whole-blood IL-10 secretion in response to cercarial excretory/secretory products. *Parasite Immunol* **35**, 147–156 (2013).
76. Baribaud, F., Pohlmann, S., Leslie, G., Mortari, F. & Doms, R. W. Quantitative Expression and Virus Transmission Analysis of DC-SIGN on Monocyte-Derived Dendritic Cells. *Journal of Virology* **76**, 9135–9142 (2002).